A QoS-Aware Energy-Efficient Chimp Optimization Routing Protocol with Efficient Sensor Node Deployment Strategy in Underwater Acoustic Sensor Network

Sambath Kumar. R.* and Sivaradje. G.

Department of ECE, Puducherry Technological University, Puducherry, India;
Email: sambath15031991@gmail.com (S.G.)
*Correspondence: shivaradje@ptuniv.edu.in (S.K.R.)

Abstract—As an extension of wireless sensor networks in the underwater environment, Underwater Acoustic Sensor Networks (UASNs) have led to a broad consideration of academicians. One of the problems that lower UWSN effectiveness in terms of network lifespan is premature energy depletion. It might be caused by the network nodes using different amounts of energy. In UASNs, the effectiveness and dependability of data transfer remain so adverse because of the intricate underwater environment in diverse ocean applications like surveilling atypical submarine oil pipelines. Inspired by the significance of UASNs' quality of service in several implementations, this study proffers a metaheuristic optimization algorithm (AG) called Chimp Optimization-based Routing Protocol (CH-ORP) for UASNs obtaining intricate features of underwater (UW) medium into concern like 3D changing topology, high propagation delay, node mobility, and density, and, also, cluster head nodes' rotation mechanism. Initially, the entire network (NW) paradigm has been considered as a three-dimensional cube out of a grid point of view, and the three-dimensional cube has been split into several little cubes by employing Delaunay Triangulation. The optimization has been carried out for lessening node failure rate and NW energy consumption rate by ideally placing the sensor nodes in UW acoustic communication. The NW topology's steadiness has been assured by the AG, and this optimizes the node redeployment scheme by computing the fitness function for all nodes. The proffered AG's simulation substantiations have been performed for exhibiting the CH-ORP's efficiency that executes finer when compared to the advanced methodologies concerning energy efficiency, reliability, and end-to-end delay. It has been found that the proposed Ch-ORP achieves 698 packets received with 28% of energy consumption, 156-sec Network delay, 257 packet loss, 97.23% of PDR, and 1256 Mbps of Network throughput.

Keywords—UASN, QoS (quality of service), routing protocol, optimization, clustering, data transfer, CH-ORP, UWE (underwater environment), RCS (relay node candidates), MFP (multifunction peripheral)

I. INTRODUCTION

Acoustic communication (AC) remains the procedure of directing and obtaining data bound by the leverage of sound propagation within the underwater (UW) environment. Data collection (DC) and collaborative observation functions have been carried out by implementing several UW autonomous vehicles (AVs) and sensors in a specific region [1]. Offshore examination, dispersed strategic surveillance applications, and oceanographic DC applications have been acquired using sensor nodes (SNs) under the sea. The UW communication (UWC) has been empowered betwixt the SNs for executing the implementations of deep-sea monitoring, unearthing resources, and ocean surveillance systems in UASN [2]. The rest of the feasible instances include Ocean Sampling Networks, pollution observation, mine reconnaissance, and the rest of the environmental surveillance like chemical, biological, and so on. Because the price, energy, and channel propagation in the UW environment (UWE) varies out of the terrestrial atmosphere [3].

High propagation delay (PD), high channel error rate, and low bandwidth remain UW acoustic channel's (AtC) few exclusive features [4, 5]. Power, processing speed, and memory space remain a few resources that can be managed by the SNs. Hence, automated DC and effortless accessibility of gathered data can be finished by evolving high-quality, effortless deployable, self-configurable, and inexpensive sensor networks within the UWE [6].

UWC's signal propagation turns into a significant issue since the communication channel remains centered upon the radio frequency [7]; hence, acoustic links [8] remain the sole reliance for UWC. Ultrasonic detection units remain equipped with onboard acoustic modems that can be used by UASNs. Additionally, the lower amount of sensor gateways (GWs) or sink nodes (SkNs) remains placed generally at the ocean surface [9]. For additional processing, UW SN gathers data and transfers this

information to the surface base station (BS) across UW AVs or multi-hop (MH) AC links [10].

The UW sensors could float because of the atmospheric features, thereby mobility modeling and node redeployment remain difficult jobs. Thus, the coverage, communication quality, and accuracy could be attained by lessening the sensor redeployment duration and price [11]. Additionally, the implementation that needs remote and swift redeployment encounters the node deployment's crucial problem. The lake's or river's water quality can be calculated through redeployed sensors within UW, and, also, this will be informed to the public by sensed data (SD) out of the UW [12, 13]. Bidimensional and tridimensional remain 2 disparate framework types in UASN [14, 15].

The sensors remaining secured to the sea's bottom remain in charge of transferring relay data to the BS where it transmits to the UW GWs through acoustic links in a two-dimensional framework [16]. For observing a provided situation, sensors and the UW AVs will be drifted at disparate depths of the three-dimensional framework. The BS monitors the data of diverse nodes' depth values [17]. The SNs' location in UASN will be discerned through a few prevailing methodologies such as node positioning algorithm (AG) [18], genetic AG [19], and, also, delay and node density-related redeployment. Herein, the ensuing objectives have been discerned: (i) to enhance effectual routing execution by establishing the QoS performance and lifespan by employing optimization AG-related routing protocol (RPl), and (ii) to lessen the communication loads and optimize energy savings providing to the prolonged lifespan of the wireless network (NW).

Owing to the environmental inconstancy, it remains vital to enhance an optimum process for SN redeployment for reflecting finer execution differences in UASN. Thus, this study's inputs include:

- Energy and QoS trade-off is attained by employing Chimp Optimization-based Routing Protocol (CH-ORP), thereby controlled data transmission (DT) assists to enhance reliability, throughput, and precision and lessens the error rate and so on.
- In this technique, DT for entire nodes has been meticulously selected centered upon the transmission link's reliability and UW SN's accessibility, which aids in lessening energy consumption (EC) in the course of DT.
- Adaptive data holding duration is computed by employing original NW for lessening PD amidst SNs in the course of transference. As well as, holding duration has been calibrated for evading collision in the NW, and this assists in enhancing NW's lifespan.

This study has been ordered as ensuing: Section I explains the background of UASN and optimization methodologies for effectual DT, Section III highlights associated studies for enhancing QoS, Section III exhibits the proffered method that encompasses NW paradigm, coverage partition (CP), optimization AG for routing procedure (RtP) and effectual DT, Segment 4 presents the experimental assessment alongside graphs by correlating 2 advanced methodologies, and, lastly, Segment 5 sums up with a conclusion and prospective study.

II. RELATED WORKS

The authors of [20] models energy augmentation RPl for enhancing energy efficiency (EE) and packet delivery ratio (PDR) in UASN by employing a hybrid CAT-Dolphin Clustering Algorithm (HC-DCA) in correlation with the Channel Aware Routing protocol. This proffered HC-DCA's execution lessens the EC (9%) and delays (7%). Analytical assessment exhibits that considerable value of energy (P=0.002; P<0.05) and delay (P=0.003; P<0.05). Inside this work's limitations, HC-DCA having quick convergence attains fine routing execution measures when correlated with CAR.

The ocean's environment and wide region turn it greatly improbable for men to analyze and observe as a difficult job and additional price than a physical task. Thus, cost-effective resolutions for surveilling and analysis implementations in the ocean remain feasible with UASN. The authors of[21] proffers a metaheuristic novel hybrid atom search heap optimization AG for optimizing the NW execution concerning energy, energy-to-energy delay (E2ED), and throughput. The NS2 simulation outcomes exhibit that this proffered study surpasses alongside prevailing Cat Optimization AG for vibrantly changing UW topology scenario.

The UASN routing strategies should, hence, consider such features for attaining balance energy, evading void holes, and enhancing NW lifespan. One of the chief problems in routing remains the void node's (VN) existence. A VN remains a node, which in no way possesses whatsoever forwarder node (FN). The void's existence might lead to bundle conveyance in the steering duration that causes data misfortune. The gap while doing steering affects the NW performance concerning proliferation delay, vitality consumption, NW lifespan, and others. Thus, by having the intention to eliminate the VN within the NWs, the authors of [22] provides an energy-efficient (E-E) optimal path routing for void prevention in UASNs. This study employs the conception of black widow optimization AG for computing the fitness function (FF), which can be employed for choosing the finest FN within the NW.

The authors of [23] incorporate localization with Normalized Advanced Factor (NAF) and Packet Delivery Probability for optimizing NW's lifetime. This NAF can be calculated out of residual energy (RE), expected transmission count, and link price. Significant simulations have been performed to assess this proffered approach and to correlate its execution with the prevailing VBF, HH-VBF, and TORA approaches. Regarding the NW having 750 nodes, this proffered approach exhibits finer execution with PDR of 95.473%, EC of 0.329 J, and mean E2ED of 2.73 s.

The authors of [24] proposed QoS-aware E-E Memetic Flower Pollination (MFP) Routing for detecting optimum E-E routing coverage set (RCS) in UW. The FF for MFP

has been devised for the Vector-based Forward protocol, which allots the dependable routing path (RP) for the source node (ScN) inside its routing pipe (RPp). This proffered AG performs in 2 phases in which Memetic AG remains in charge of detecting the optimum RCS, and FPA remains in charge of substituting betwixt local and global pollination to send packets in dependable RP. Also, this proffered study regards Grant Free Pattern Division Multiple Access packets for RtP as this lessens the latency at the packet transmission time.

The authors of [25] highlights a routing named Inter-Intra Cluster Energy Balanced Routing protocol (IICEBRP) that is applied for UASN for surpassing latency and the rest of the intervention for balancing the energy for the whole NW. This RPl proffered for energy balancing betwixt the nodes has been employed for communicating the SD. This NW coding application remains inter and intra-cluster for attaining the requirements of lessening the EC of the node and prolonging the NW's lifespan. The result exhibits that this proffered IICEBRP could discharge the failure frequency within the node, discern each node's EC, and effectually prolong the NW's lifespan.

The authors of [26] presents a Q-learning-based MH cooperative routing (QL-MHCR) protocol for UWSNs. This could automatedly select nodes having the maximal Q-value as forwarders centered upon distance data. Additionally, this study joins cooperative communications with Q-learning AG for lessening NW EC and enhancing communication effectiveness. Experimental outcomes exhibit that QL-MHCR's running duration remains below 1/10th of that of the artificial fish-swarm AG, whereas the routing EC remains maintained at a similar level.

The authors of [27] puts forth a mobility prediction (MP) optimal data forwarding protocol for UASNs centered upon MP. Rather, by regarding an attainable and manually motivated mobility paradigm, this protocol prospers to send each produced data packet (DP) via a single finest path devoid of the requisite to interchange notification messages owing to the MP module.

The authors of [28] presents a new chaotic search-and-rescue-optimization-based MH DT (CSRO-MHDT)

protocol for UWSNs. While employing this approach, cluster heads (CHs) have been chosen and clusters have been pre-ordered portraying various features incorporating RE, intracluster distance, and intercluster detachment. Also, the CSRO AG has been addressed that has been generated by integrating chaotic conceptions into the traditional SRO AG. Additionally, this technique computes an FF, which considers RE, distance, and node degree amidst the rest of the features. This study's unique feature has been signified by the CSRO AG's formulation for route optimization that has been evolved in-house.

The authors of [29] provide UWSN-related occurrences surveillance implementations. This proffered FFRP strategy in the course of events data collection uses a self-learning-based dynamic gathering mating optimization intelligence for seeking the greatly stabilized and dependable RPs to routing packets surrounding connectivity voids and shadow zones within UWSNs. This proffered strategy while communicating data lessens the increased EC and latency problems by equalizing the data traffic load (DTL) equivalently in a wide-range NW. Furthermore, the DT through greatly steady links betwixt acoustic nodes (ANs) enhances the comprehensive PDR and NW throughput in UWSNs.

The authors of [30] introduce a new QoS-aware evolutionary cluster-based routing protocol (QAECRP) for UWSN-related implementations. This enhances PDR and lessens mean E2ED and comprehensive NW EC. This study's correlative execution analyses exhibit that QAECRP remains effective in attaining less NW delay, increased PDR, and less EC.

From the recent protocols' review, it has been noticed that enhanced delay and energy drainage remain 2 vital domains, which require additional resolutions. Next, an easy-to-implement RPl has been designed, which could assure EE alongside lessened delay to diverse implementations deployed in UASNs

III. PROPOSED METHODOLOGY

This proffered study regards static multiple SkNs for gathering the ocean floor data.
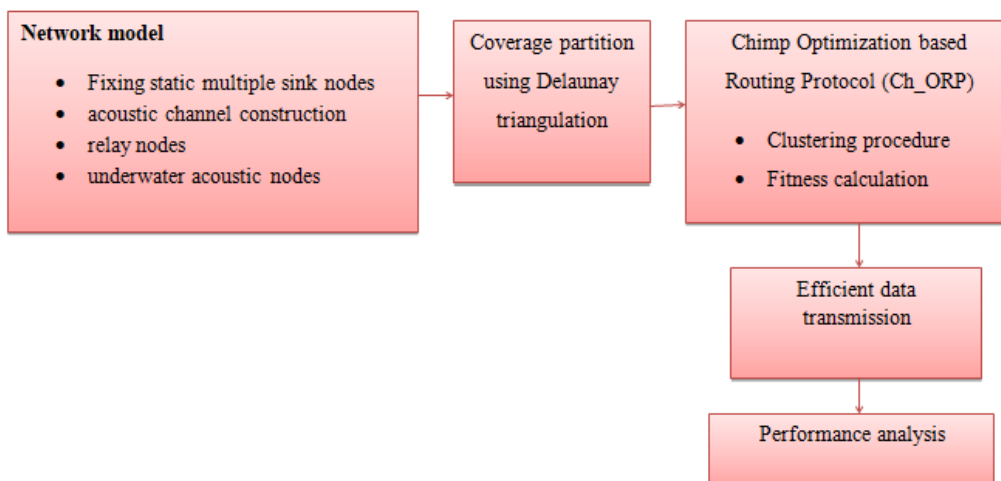

Figure 1. Proposed Methodology of CH-ORP.

In the prevailing paradigm, it has been observed that nodes adjacent to the sink lose their energy shortly and perish because of dealing with large traffic loads. For surpassing this, replaceable relay nodes (RyNs) have been deployed adjacent to multiple sinks, as illustrated in Fig. 1.

The power source within the UW SN contains a battery having limited energy, and this has not been attainable for energizing the battery often. Hence, routing must be watched out efficiently for preventing the inessential activity of multiple sensors UW. In Delaunay Triangulation (DyT), a routing radius has been generated out of ScN to sink, and the nodes within the RPp remain qualified to forward its DP to the sink. When the RPp integrates dense SNs, entire SNs' energy would be employed for forwarding the repetitious source DP, which leads to redundant energy waste in DyT. For evading these limitations and for enhancing UASN's lifespan, this study proffers a QoS-aware data delivery procedure in harsh UWE. This proffered system focuses on providing CH-ORP for detecting the optimal RCS in order that the ScN covers entire RyNs. Furthermore, flower pollination AG has been employed for substituting betwixt RCSs and selecting the reliable path for reaching the sink

A. Network Paradigm

There remain multiple criteria, which influence the propagation of acoustic signal (AS), traffic execution, and EC in UWE. In UASN, the Thorp propagation (TpP) paradigm has been employed for defining the AtC's features in UASN. Relying upon the features, which influence the AS's execution, the paradigm for attenuation over AtC has been provided by,

$$A(d,f) = d^k a(f)^d \qquad (1)$$

in which d represents the distance betwixt the transmitter and receiver where the attenuation in AtC has been noticed, ($k = 1.5$) represents the geometric spreading, and $\alpha(f)$ represents the coefficients of absorption (CoA). The TpP paradigm has been employed for devising the CoA $\alpha(f)$, that has been provided as

$$\alpha(f) = \begin{cases} 0.03 + 2.75 \times 10^{-4} f^2 + \frac{0.12f^2}{1+f^2} & f \geq 0.4 \\ 0.002 + 0.11f^2 + \frac{0.121}{1+f^2} & f < 0.4 \end{cases} \qquad (2)$$

$$N(f) = N_t(f) + N_w(f) + N_s(f) + N_{th}(f) \qquad (3)$$

in which $N_{th}(f)$ portrays the position in the sequence of frequency and $N_t(f)$ portrays the noise generated because of turbulence that has been provided by $10 \log(N_t(f)) = 17 - 30 \log(f)$, $N_s(f)$ portrays the noise generated because of ship traffic that has been provided by $10 \log(N_s(f)) = 40 + 10(2s - 1) + 26 \log(f) - 60 \log(0.03 + f)$. $N_w(f) 10 \log(N_s(f)) = 40 + 10(2s - 1) + 26 \log(f) - 60 \log(0.03 + f)$. $N_w(f)$ portrays the noise generated because of

thermalor heat actions that have been provided by $10 \log(N_{th}(f)) = -15 + 20 \log(f)$.

Relying upon the signals' propagation distance (d) and frequency (f) within the UWE, the SNR at the receiver has been portrayed by

$$snr(f,d) = p(f) - A(d,f) - N(f) - TL(d) + DI \geq DT \qquad (4)$$

in which DT indicates the receiver identification threshold, and DI indicates the directive index. $P(f)$ indicates the transmission power (TP) acquired at the transmitter that relies on transmitted signal intensity (TSI) (I_T), depth of NW (DNW) (H), and E2ED (d). Next,

$$I_T = 10^{p(f)/10} \times 0.67 \times 10^{-18} \qquad (5)$$
$$P_{TS}(d) = 2\pi h \times I_T \qquad (6)$$
$$P_{TS}(d) = 4\pi I_T \qquad (7)$$
$$P_T(d) = P_{TS}(d) + P_{Td}(d) \qquad (8)$$

Eq. (8) exhibits that, when SNR remains at least the value of threshold DT, the received signals could be identified at the receiver devoid of whatsoever error. Thus, the TP has been fixed progressively centered upon signal frequency (f), propagation distance (d), and the rest of the features such as TSI, DNW, and E2ED for lessening the EC to enhance the NW's lifespan.

B. Coverage Partition by Employing Delaunay Triangulation

For enhancing the sensor deployment issues bound by disparate scenarios, it is presumed that the surveillance region has a 2D plane. The wireless SNs embrace the Boolean sensing model (BSM), that is, the target point's probability in the sensing range (SsR) remains one; or else, this remains zero for simplifying the coverage issue. If the sensors' quantity remains more, the entire nodes' sum coverage rate (CR) to the surveillance region remains arduous to be resolved by formulation. Hence, the area has been split into grid points of equivalent dimension that could be added equal to pels having a distinct accuracy of one. The general SsR remains as a disk based on the SNs' position. The BSM could be defined arithmetically as the SN's coordinates $s_i = (x_i, y_i)$, and the sensing radius (SR) has been in a configured Euclid space at this time. Next, the pixel point's (PP) probability alongside coordinates that could be observed as

$$p(a, s_i) = \begin{cases} 1, d(a, s_i) \leq R_i \\ 0, otherwise \end{cases} \qquad (9)$$

in which the Euclid distance $d(a, s_i) = /a, s_i/$. Notice that the sensor set $S = \{s_i\} i = 1, \dots, M$. PP a might be observed by disparate sensors; hence, its overall perception probability remains,

$$p(a, s) = 1 - \prod_{s_i \in S} [1 - p(a, s_i)] \qquad (10)$$

The aforementioned description of the CR remains the chief common intended action for optimum sensors' deployment. For K-coverage (KC) issues with disparate necessities, solely specified limitations are required to be included. If this remains an unlimited coverage optimization issue, this depicts that few chief objectives should be incorporated, and this might possess KC limitation having specified NW lifetime scenarios for assuring that every significant point should lie inside the coverage range of K SNs. For employing the DyT as a WSN coverage metric tool, two rules have been included prior to producing the DyT graph. The initial rule includes additional sensors at the field corners (FCs) and the presumed convex of the outer polygon (OPg) of the coverage paradigm might not incorporate the entire field. As the OPg in DyT remains consistently convex, extra sensors on the FCs result in the field's complete triangulation. Next, when 3 sensors could not generate a triangle since these remain collinear, one of these has been moved by a haphazard multiple of 0.5 m for allowing the DyT to generate a triangle.

The region divided by Delaunay remains a triangular NW containing triangles N_Δ having diverse figures as illustrated in Fig. 2. Subsequent to the completion of computations, in region L, the triangles' quantity N_Δ relies upon the location coordinate (LC) $s_i(x_i, y_i, z_i)$ of the node and the nodes' quantity n. Therefore, the nodes' higher quantity means the generation of additional triangles N_Δ. At first, the haphazardly deployed nodes' quantity in regions like 200 and 500 DyT acquires out of the test remained $N_\Delta = 184$. Next, the sum region s_0 of the created Delaunay graph as well as modifies alongside the nodes' quantity and LC as illustrated in Figure 3. As a result, as the nodes' quantity n rises, the sum area s_0 of Delaunay as well as rises, and its area proportion $\frac{s_0}{s_l}$ steadily reaches a hundred percent.
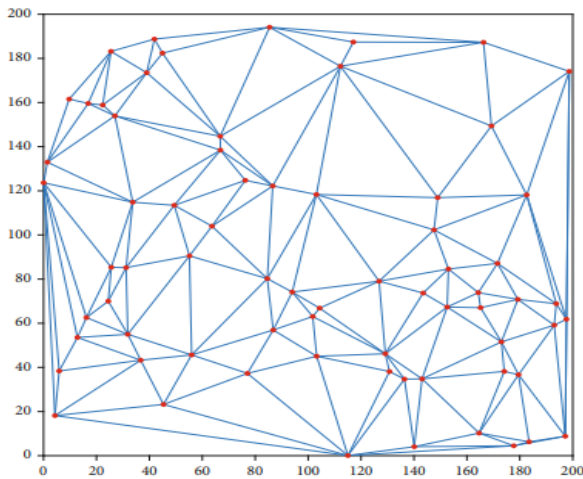

Figure 2. 2D Delaunay division.

Initially, the known nodes' (KNs) quantity n remains haphazardly deployed in a plane having a region of L dimension. Next, the correlating DyT has been produced

as per the KNs' LCs $s_i(x_i, y_i)(i = 1,2, \ldots, n)$. Hence, in the initial phase, the judgment methodology has been employed for determining a triangle enclosed by T. Then, the inner coordinates (ICs) $s_j(x_j, y_j)$ correlating to every Delaunay triangle (DlT) have been computed and produced. The coordinates of the triangle's inner point could be computed by

$$s_j(x_j, y_j) = \left(\frac{(a_ix_i + b_ix_{i+1} + c_ix_{i+2})}{(a_i + b_i + c_i)}, \frac{(a_iy_i + b_iy_{i+1} + c_iy_{i+2})}{(a_i + b_i + c_i)}\right) \quad (11)$$

in which a_i, b_i, and c_i denote the triangle's side lengths, and (x_i, y_i), (x_{i+1}, y_{i+1}), and (x_{i+2}, y_{i+2}) denote the triangle's vertices correlating to the inner center. Centered upon this methodology, the triangle enclosed by the target and its correlating ICs have been discerned. Then the area proportion $s_k = s_j/s_m$ of the triangle to which the target $T_f(x_f, y_f)$ corresponds has been computed. The entire triangle's area has been presumed as $s_j, j = 1,2,3, \ldots N_\Delta$, and the median $s_m = (s_{\frac{j+1}{2}} + s_{\frac{j}{2}}, j = 1,2,3, \ldots, N_\Delta)$ triangle's area has been acquired. When $s_j \leq s_m$, the triangle's IC $G_j(x_j, y_j)$ has been regarded to be the target's predicted coordinate. When $s_j > s_m$, the vertices of the triangle's are being used as the predicted value of T.

Optimal SR (OSR) has been computed for every triangle, and, thus, the quadratic sensing paradigm has been fine-tuned krs^2 in which, rs^2 remains the SR, and k remains the constant. It is exhibited that the 3 sensors' EC at every triangle's vertex has been lessened while their sensing discs intersect the triangle's circumcenter $\sum_{j=1}^{3} x_j /3, \sum_{j=1}^{3} x_j /3$. The OSR has been functioning as

Phase i – Every sensor computes the OSR for every of its neighboring DlTs.

Phase ii – Every sensor selects the highest OSR amidst those computed in phase i.

C. Proffered CH-ORP

The CH-ORP remains a swarm intelligence program influenced by the chimp's natural hunting mechanism. The 4 classes of agents in their community remain the driver, barrier, chaser, and attackers. Although every chimp in a folk has distinct capabilities, these variations will be needed for precisely shaping the hunting process (HP). The paradigm of the driver and chaser has been arithmetically classified by,

$$X_{chimp}^{(t+1)} = X_{prey}^t - 1 | c.X_{prey}^t - m.X_{chimp}^t | \quad (12)$$

in which X_{prey}^t and X_{chimp}^t represent the position vectors of the prey and chimp, t represents the current iteration (CI), and a, m, and c represent the coefficients indicated as,

$$a = 2.f.rand_1 - a \quad (13)$$

$$c = 2.rand_2 \quad (14)$$

$$m = chaotic\_value \quad (15)$$

In the above expressions, f remains nonlinearly lowered over iterations within the range [2.5, 0], whereas $rand_1$ and $rand_2$ remain the values betwixt zero and one; the *m* vector conveys the sexual desire of agents by employing diverse chaotic vectors. The CH-ORP starts with the stochastic populace generation of agents. This phase remains just like the rest of the swarm-related techniques wherein the first gathering of agents should continuously have emerged in the course of iterations. The agents have been haphazardly designated to 1 of the 4 classes – driver, barrier, attacker, or chaser. Every group's plans and schemes would be described in what way the agents' positions have been updated by seeking the *f* vector, whereas entire groups would try to anticipate the finest prey locations. The prey posture remains the finest until then. The *c* and *m* vectors have been changed during iterations that enhance local minima (LM) prevention and meeting swiftness. The attacker chimp guides the exploitation stage, and the rest of the agents could haphazardly join the HP. As the prey's optimum location could not be initially discerned, the finest-acquired resolutions have been utilized for stimulating the HP arithmetically. The initial driver, attacker, chaser, and barrier chimps have been considered the finest agents, and the rest agents modify their positions respectively. The ensuing expression portrays the location updating rule:

$$x_1 = x_{attacker}^t - a_1|c_1 x_{attacker}^t - m_1 x^t| \quad (16)$$

$$x_2 = x_{barrier}^t - a_2|c_2 x_{barrier}^t - m_2 x^t| \quad (17)$$

$$x_3 = x_{chaser}^t - a_3|c_3 x_{chaser}^t - m_3 x^t| \quad (18)$$

$$x_4 = x_{driver}^t - a_3|c_3 x_{driver}^t - m_4 x^t| \quad (19)$$

$$x(t+1) = \frac{x_1 + x_2 + x_3 + x_4}{4} \quad (20)$$

$$X_{chimp}^{(t+1)} = \begin{cases} X_{prey}^t - a.d & if\ \mu < 0.5 \\ chaotic_{value} & if \geq 0.5 \end{cases} \quad (21)$$

where x_1, x_2, x_3, x_4 indicates that variable of $x_{attacker}^t$, $x_{barrier}^t$, x_{chaser}^t, x_{driver}^t raised to the power being calculated by the time "T.

In which μ indicates a random number (RN) inside the range [0, 1]. Consequently, CH-ORP has been at first established by the generation of haphazard agents (candidate solutions). Next, entire agents have been categorized into 1 of the 4 independent groups described formerly. Ensuing this, agents update their f vector by employing the classified scheme provided to them. Ensuing this, the 4 classes analyze the possible prey sites alongside every cycle. Next, the distances of agents and preys could be updated. Furthermore, the c and m tuning criteria lead to the prevention of LO and a quicker convergence rate. Lastly, CMs facilitate the convergence speed to be increased when avoiding LM stagnancy.

D. Starvation Mode

The searching agents' (SAs) starvation has arithmetically emerged with μ_1 and μ_2 by,

$$\mu_1(\tau) = \begin{cases} hungry\ (i).\frac{N}{SHungry} \times r_4, r_3 < \tau \\ 1, r_3 > \tau \end{cases} \quad (22)$$

$$\mu_2(\tau) = (1 - \exp(-|hungry\ (i) - Shungry| \times r_5 \times 2 \quad (23)$$

In the above expression, every SA's hunger value and entire SAs' hungry feelings' total have been accordingly portrayed by *Hungry* and *SHungry* (*sum(hungry)*), *N* indicates SAs' quantity, and r_3, r_4, and r_5 indicates RNs within the range of [0, 1]. The $hun(i)$ has been defined as,

$$hungry\ (i) = \begin{cases} hungry\ (i) + H, allfitness\ (i) = BF \\ 0\ all\ fitness\ (i) == BF \end{cases} \quad (24)$$

Every SA's fitness stores in $allfit\ (i)$ for the CI, and *H* could be derived by,

$$H = \begin{cases} TH & TH \geq LH \\ LH \times (1 + r) & TH < LH \end{cases}, TH = \frac{F(i) - BF}{WF - BF} \times 2 \times r_6 \times$$

$$(UB - LB) \quad (25)$$

in which $F(i)$ portrays every SA's fitness value, r_6 portrays an RN within the range of [0, 1], BF portrays the finest FV computed in the CI, WF portrays the poorest fitness computed in the CI, and LB and UB portray the search space's lesser and higher bounds accordingly.

E. CH-ORP Clustering Process

Consider *R* signifies the SNs spread haphazardly surrounding the area and grouped into Nc clusters. The mentioned equation indicates the CH vector as a searching agent generated by the SN. This CH coordinates communication amidst cluster nodes, gathers intra-cluster data, and communicates through RyN in this manner. CHs have been selected centered upon the nodes' location and energy level (EL). For forming clusters having nodes of similar quantity, the BS would be induced to allocate CHs with optimum placements and high residual work. Consequently, this approach could be considered as an optimization job, wherein its FF has been exhibited as,

$$F_{CH} = \beta \times f_{energy}^{CH} + (1 - \beta) \times f_{location}^{CH} \quad (26)$$

As depicted in the above equation, F_{CH} incorporates 2 components - f_{energy}^{CH} and $f_{location}^{CH}$ - wherein the β constant exhibits every component's input to the FF, that is, F_{CH}; f_{energy}^{CH} signifies CHs' mean residual work (MRW) divided by non-CH nodes' (N-CHNs) MRW, and this has been described by,

$$f_{energy}^{CH} = \frac{E'_{CH}}{E_{CH'}} = \frac{\sum_{\propto node_j \in CH} E_{CH}^{residual}(j)/|CH|}{\sum_{\propto node_j \in CH'} E_{CH'}^{residual}(j)/|CH'|} \quad (27)$$

in which E'_{CH} portrays the MRW executed by the CH, $E_{CH'}$ portrays the MRW executed by the N-CHNs, $|CH'|$ and $|CH|$ portray the N-CHNs' and CH nodes' quantity, accordingly. It must be noticed that f_{energy}^{CH} has been employed for selecting the CHs out of nodes having the greatest ELs, and $f_{location}^{CH}$ remains the maximal distance betwixt N-CHNs and BS divided by the mean distance betwixt BS and CHs as,

$$f_{location}^{CH} = \frac{D'_{CH}}{D_{CH'}} = \frac{\sum_{\propto node_j \in CH} d(node_i, base\ station)/|CH'|}{\sum_{\propto node_j \in CH'} d(node_j, base\ station)\overline{|CH|}} \quad (28)$$

in which $d(node_i, base\ station)$ depicts the Euclidean distance betwixt $node_i$ and base station. $f_{location}^{CH}$ has been proffered for deciding the optimal cluster generation and CHs for a standard UWSN for enhancing its EE. It remains just natural that power production could discern a node's anticipated lifespan. This information could be integrated into the data.

F. Routing Process

Every outcome exhibits a match betwixt a solo entrance and a BS. For entire GWs, the findings' dimension remains the same (Q). The solution expresses the path from every GW to the BS in the manner that every GW begins with an RN:

$$G_{p,q} = rand(0,1), 1 \leq p \leq N_i, 1 \leq q \leq Q \quad (29)$$

in which, the component q indicates the solution's GW number, and N_i indicates the initial solution; next, it would define the GW lz and the route from lp to the BS, exhibiting which lq transmits data to lz. Eq. (30) defines the path's finding map:

$$I_z = Idx\left(SetN \times tL(I_q). Ceil(G_{p,q} \times |SetN \times tL(I_q)|)\right) \quad (30)$$

where I_z defines the variable, SetN refers the elements of nodes in network, $tL(I_q)$ refers time related value associated with I_q, $G_{p,q}$ represents the function variable of p and q.

The FF calculates the solutions' merit concerning the variables that they possess, and Idx represents an indexing function employed for computing the n GW's index. FFs have been currently present for creating an appropriate RP betwixt every GW and BS. Typically, Eq. (31) presents the distance (D) traversed by gates, whereas Eq. (32) defines the GWs over the whole NW.

$$D = \sum_{q=1}^{Q} dst(I_p, N \times tL(I_p)) \quad (31)$$
$$G_N = \sum_{p=1}^{N} NxtL \times Count(I_p) \quad (32)$$

The shortest distance dst has been covered, and the fewest hops I_p remain the criteria for routing. As a result, the larger the fitness value for the outcome, the shorter the overall distance traversed, and the fewer hops, i.e., lengths L and hops I_p are inversely proportional to the routing fitness function's value. The population's optimal searching agent is the candid solution with the highest fitness value. The fitness function is formulated using

$$Routing - fitness = \frac{\theta}{\theta_1 \times D + \theta_2 \times G_N} \quad (33)$$

$$\theta_1, \theta_2 \in [0,1], \theta_1 + \theta_2 = 1, \theta: Proportionality\ Constant \quad (34)$$

Routing fitness' significant feature remains to assure that entire distances and the hops' quantity within the NW would be equivalently dispersed.

G. Effectual DT to Enhance QoS

Subsequent to the optimization-related RtP, data holding duration could be predicted centered upon nodes' waiting and discovering time existing within the NW and the DT level in the course of forwarding control that is computed by employing a QoS-aware queuing paradigm. In QoS-aware designing, appropriate hop selection has been analyzed centered upon reliability sensitivity packets (RSP) and ordinary packets (OP). In the QoS metrics, the queue has been analyzed in 2 classes in which, when the $RSP > OP$, the DPs would be sent on condition that when the queue has been nullified or emptied. When the RSP flops to send the data to the UW area's SNs, OP considers sending the data to the correlating node through GW for matching QoS for reliable DT having low EC.

When the packets are acquired centered upon RSM and OP, the packets within the buffer are computed centered upon "request/reply" controls in the buffers centered upon adaptive data hold rate (ADHR) assessment as,

$$Ncost\ (\epsilon)_{ij} = \frac{source_{id}, request_{id}\ from\ j}{sink_{id}\ from\ j\ to\ L} \quad (34)$$

in which "i, j" $->$ appears as the node within UASN in which, centered upon the request control, the subsequent feasible hop has been detected by the "i" node having ADHR according to the reply response out of the node "j" node. Out of this discourse, the link quality and accessibility could be enhanced via data hold rate (DHR) and augmenting delay within the saved packets' NW as depicted in the following equation:

$$A_D = \frac{1}{N} \sum_{A=1}^{N} T_C - T_A \quad (35)$$

in which A_D indicates the mean delay alongside the total current time and arrival time that is portrayed as $T_C - T_A$. The difference has been analyzed at "N^{th}" items saved within the buffers. When data is saved, that is, hold rate time within the buffer remains elevated, it results in rising the data reliability that has been

computed centered upon service request time as depicted in the following equation:

$$cost\ (\in)_{SR} = \frac{N(packets\ in\ buffer)}{rate\ of\ service\ (R_s)} \qquad (36)$$

The buffer time $cost\ (\in)_{SR}$ has been computed centered upon the data rate (DR) proportion at the buffer in the queue with the different betwixt *cost*. Thus, efficient DR has been managed and sustained by employing adaptive service rate and arrival rate related to hop counts (min and max values). When the PD rises alongside the hop count, it assists in compensating the DHR and lessening the data loss within UASN. Out of this discourse, the ''request'', ''reply'', and ''data'' packets are computed as,

$$f(x) = \begin{cases} time_{rq} + time_{rp} + time_{data} + 3Xtime_p & request \\ time_{rp} + time_{data} + 2XT_p \end{cases} \qquad (37)$$

in which

$time_{rq}$ is Time needed for SN

$time_{rp}$ is Time needed for forwarder

$time_{data}$ is Time needed for the sensor for saved data

$time_p$ is Propagation time

In this adaptive technique, in the course of every transfer, the DPs have been summed within the buffer that avoids unnecessary transfer for lessening collision within the UASN for reliable DT.

IV. RESULTS AND DISCUSSION

A. Performance Analysis

This segment assesses and correlates the execution of Various RPls for UWSNs. The assessment involves correlating the execution of these protocols and analyzing their performance with QoS-aware Evolutionary Cluster-based method.

TABLE I. PACKETS RECEIVED CORRELATION

Time (s)	QERP	FFRP	EESFL	NADIR	EEM CCP	CH-ORP
20	45	81	154	186	210	274
40	96	125	184	206	257	327
60	157	175	247	271	328	457
80	196	234	268	296	371	527
100	245	296	324	385	458	698

Routing Protocol (QERP) and Firefly Mating Optimization Routing Protocol (FFRP), Energy-Efficient Secure Fuzzy Logic-based Cross-Layer design routing protocol (EESFL), Network-Aware aDaptIve Routing (NADIR), Energy-Efficient Minimum Cost Cluster protocol (EEMCCP) strategies concerning diverse criteria. Table-1 shows the packets received correlation for various methods with a period between 20 sec to 100 sec.
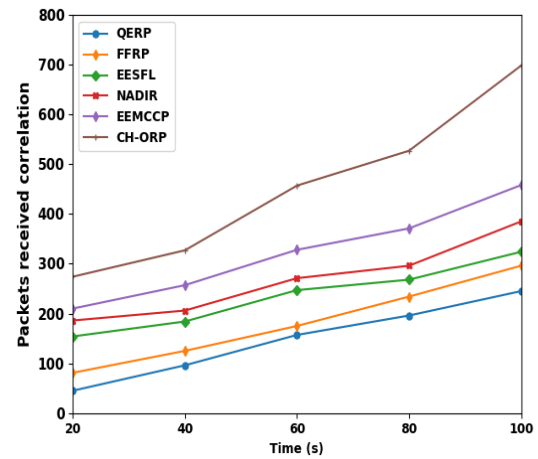

Figure 3. Packets received correlation.

Fig. 3 illustrates the packets received (PR) correlation of prevailing QERP, FFRP, EESFL, NADIR, EEMCCP, and the proffered CH-ORP. The X-axis and Y-axis indicate the time in seconds and the values attained in kbps accordingly. While correlated, prevailing QERP, FFRP, EESFL, NADIR, and EEMCCP methodologies attain 245kbps, 296kbps, 324kbps, 385kbps, and 458 kbps of PR, whereas the proffered CH-ORP methodology attains 698kbps of PR. Table II shows energy consumption for various methods with a period between 20 sec to 100 sec.

TABLE II. EC CORRELATION

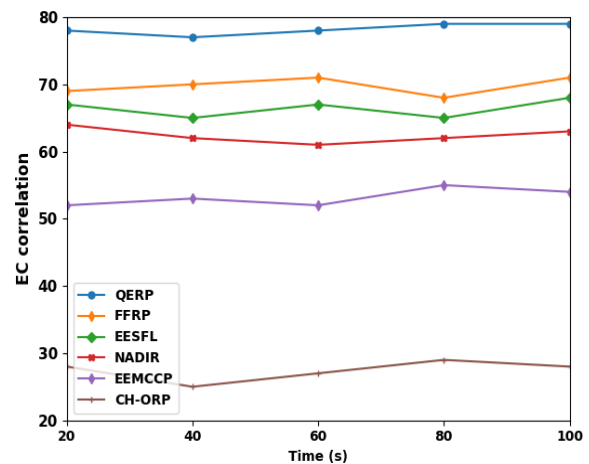| Time (s)	QERP	FFRP	EESFL	NA DIR	EEM CCP	CH-ORP
20	78	69	67	64	52	28
40	77	70	65	62	53	25
60	78	71	67	61	52	27
80	79	68	65	62	55	29
100	79	71	68	63	54	28

Figure 4. EC correlation.

Fig. 4 illustrates the EC correlation of prevailing QERP, FRP, EESFL, NADIR, EEMCCP, and the proffered CH-ORP. The X-axis and Y-axis indicate the

time in seconds and the values attained in percentage accordingly. While correlated, prevailing QERP, FFRP, EESFL, NADIR, and EEMCCP methodologies 79%, 71%,68%,63%, and 54%, and 458 kbps of EC, whereas the proffered CH-ORP methodology attains 28% of EC. Table III shows the network delay correlation for various methods with a period between 20 sec to 100 sec.

TABLE III. NETWORK DELAY CORRELATION

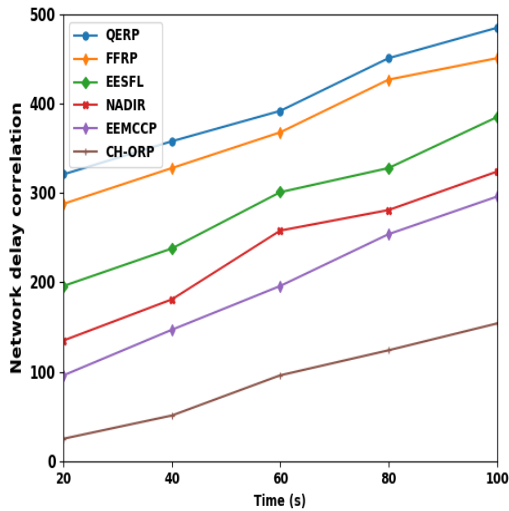| Time (s)	QERP	FFRP	EESFL	NADIR	EEMCCP	CH-ORP
20	321	288	196	135	96	25
40	358	328	238	181	147	51
60	392	368	301	258	196	96
80	451	427	328	281	254	124
100	485	451	385	324	296	154

Figure 5. Network delay correlation.

Fig. 5 illustrates the network delay (ND) correlation of prevailing QERP, FRP, EESFL, NADIR, EEMCCP, and the proffered CH-ORP. The X-axis and Y-axis indicate the time in seconds and the values attained in kbps accordingly. While correlated, prevailing QERP, FFRP, EESFL, NADIR, and EEMCCP methodologies 485kbps, 451kbps, 385kbps, 324kbps, and 296 kbps of ND, whereas the proffered CH-ORP methodology attains 154kbps of ND. Table-4 shows the packet loss correlation for various methods with a period between 20 sec to 100 sec.

TABLE IV. PACKET LOSS CORRELATION

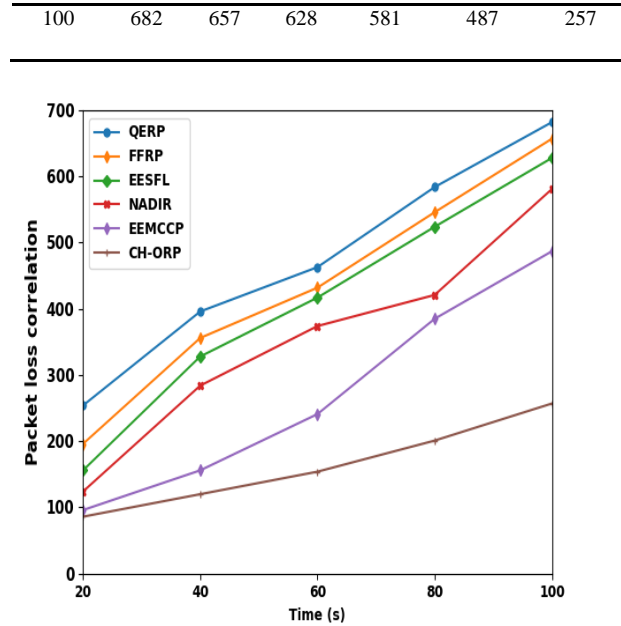| Time (s)	QERP	FFRP	EESFL	NADIR	EEMCCP	CH-ORP
20	254	196	156	124	96	86
40	396	356	328	284	156	120
60	463	432	417	374	241	154
80	584	546	524	421	385	201
100	682	657	628	581	487	257

Figure 6. Packet loss correlation.

Fig. 6 illustrates the packet loss (PL) correlation of prevailing QERP, FRP, EESFL, NADIR, EEMCCP, and the proffered CH-ORP. The X-axis and Y-axis indicate the time in seconds and the values attained in kbps accordingly. While correlated, prevailing QERP, FFRP, EESFL, NADIR, and EEMCCP methodologies 682kbps, 657kbps, 628kbps, 581kbps, and 487kbps of PL, whereas the proffered CH-ORP methodology attains 257kbps of PL. Table-5 shows PDR for various methods with a period between 20 sec to 100 sec.

TABLE V. PDR CORRELATION

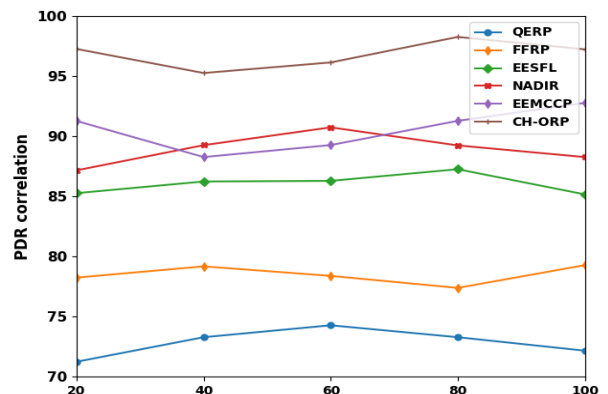| Time (s)	QERP	FFRP	EESFL	NADIR	EEMCCP	CH-ORP
20	71.25	78.25	85.27	87.17	91.27	97.26
40	73.29	79.18	86.24	89.26	88.27	95.26
60	74.28	78.39	86.29	90.74	89.27	96.14
80	73.29	77.39	87.26	89.24	91.28	98.26
100	72.17	79.28	85.17	88.27	92.78	97.23

Figure 7. Network delay correlation

Fig. 7 illustrates the PDR correlation of prevailing QERP, FRP, EESFL, NADIR, EEMCCP, and the proffered CH-ORP. The X-axis and Y-axis indicate the time in seconds and the values attained in percentage accordingly. While correlated, prevailing QERP, FFRP, EESFL, NADIR, and EEMCCP methodologies 72.17%, 79.28%, 85.17%, 88.27%, and 92.78% of PDR, whereas the proffered CH-ORP methodology attains 97.23% of PDR. Table VI shows network throughput for various methods with a period between 20 sec to 100 sec.

TABLE VI. NETWORK THROUGHPUT CORRELATION

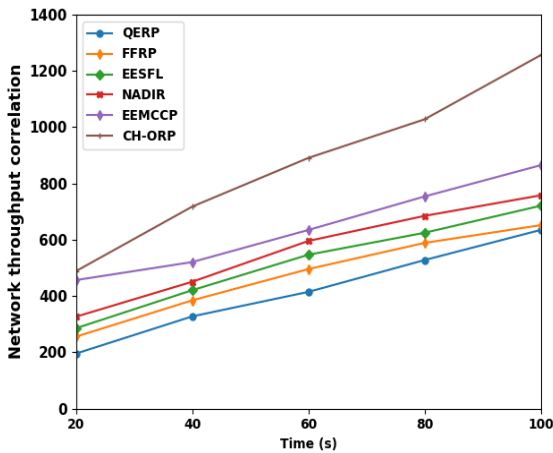| Time (s)	QERP	FFRP	EESFL	NADIR	EEMCCP	CH-ORP
20	196	256	286	327	457	489
40	328	385	421	451	521	718
60	415	496	547	596	635	891
80	528	589	625	685	754	1028
100	635	652	721	758	865	1256

Figure 8. Network throughput correlation

Fig. 8 illustrates the network throughput (NT) correlation of prevailing QERP, FRP, EESFL, NADIR, EEMCCP, and the proffered CH-ORP. The X-axis and Y-axis indicate the time in seconds and the values attained in percentage accordingly. While correlated, prevailing QERP, FFRP, EESFL, NADIR, and EEMCCP methodologies achieve 635kbps, 652 kbps, 721kbps, 758kbps, and 865kbps of NT, whereas the proffered CH-ORP methodology attains 1256kbps of NT.

TABLE VII. COMPREHENSIVE CORRELATIVE ASSESSMENT

Criteria	QERP	FFRP	EESFL	NADIR	EEMCCP	CH-ORP
PR	245	296	324	385	458	698
EC	79	71	68	63	54	28
ND	485	451	385	324	296	154
PL	682	657	628	581	487	257

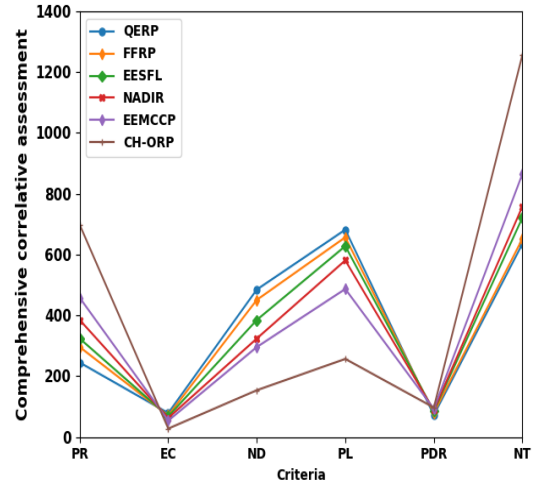|						
PDR	72.17	79.28	85.17	88.27	92.78	97.23
NT	635	652	721	758	865	1256

Figure 9. Comprehensive correlative assessment.

Fig. 9 illustrates the Comprehensive correlative assessment of prevailing QERP, FRP, EESFL, NADIR, EEMCCP, and the proffered CH-ORP. The X-axis and Y-axis indicate the time in seconds and the values attained in percentage accordingly. While correlated, prevailing QERP, FFRP, EESFL, NADIR, and EEMCCP methodologies achieve 635kbps, 652 kbps, 721 kbps, 758 kbps, and 865 kbps of NT, whereas the proffered CH-ORP methodology attains 1256 kbps of NT.

V. CONCLUSION

Modeling an RPl for E-E and reliable data collection remains the chief consideration in UASNs. This study proffers a new and effective chimp optimization-based routing strategy for UASNs-related time-critical marine surveillance implementations. This established procedure in the course of data collection occurrences uses a self-learning-related dynamic optimization intelligence for searching the greatly steady and reliable RPs for expressing collected data in voids of shadow zones within UASNs. This modeled strategy considerably lessens EC, latency, and LO problems by equalizing the DTL equivalently within the NW. Furthermore, the DT over greatly steady links betwixt ANs enhances the PDR and throughput in UASNs.

CONFLICT OF INTEREST

The authors declare no conflict of interest with this research article.

AUTHOR CONTRIBUTIONS

Sambath Kumar. R contributed for the proposed methodology work, software, conceptualization and acquisition of data or analysis, interpretation of data. Sivaradje. G has done drafting the work and revising it

for important contents. All authors had approval the final version.

REFERENCES

[1] K. M.Awan, P. A. Shah, K. Iqbal, S. Gillani, W. Ahmad, and Y. Nam, "Underwater wireless sensor networks: A review of recent issues and challenges,"*Wireless Communications and Mobile Computing*, pp. 1–20, 2019.

[2] A. Khasawneh, M. S. AbdLatiff, O. Kaiwartya, and H. Chizari, "A reliable energy-efficient pressure-based routing protocol for underwater wireless sensor network," *Wireless Networks*, vol. 24, no. 6, pp. 2061–2075, 2018.

[3] K. S.Geethu and A. V. Babu, "Minimizing the total energy consumption in multi-hop UWASNs,"*Wireless Personal Communications.*, vol. 83, no. 4, pp. 2693–2709, 2015.

[4] R.B.Manjula andS.S. Manvi, "Coverage optimization based sensor deployment by using PSO for anti-submarine detection in UWASNs,"in *Proc. 2013 Ocean Electronics (SYMPOL) IEEE*, pp. 15–22, 2013.

[5] G.Han, J. Jiang, N. Sun, and L. Shu, "Secure communication for underwater acoustic sensor networks,"*IEEE Communications Magazine*, vol. 53, no. 8, pp. 54–60, 2015.

[6] N. Z.Zenia *et al.*,"Energy-efficiency and reliability in MAC and routing protocols for underwater wireless sensor network: A survey,"*Journal of Network and Computer Applications*, vo. 71, pp. 72–85 2016.

[7] L.Karim, Q. H.Mahmoud,N. Nasser, A. Anpalagan, and N. Khan, "Localization in terrestrial and underwater sensor-based m2m communication networks: Architecture, classification and challenges,"*International Journal of Communication Systems*, vol. 30, no. 4, 2017.

[8] J.Wang, W. Shi, L. Xu, L. Zhou, and Q. Niu, "Design of optical-acoustic hybrid underwater wireless sensor network," *Journal of Network and Computer Applications*, vol. 92, pp. 59–67, 2017.

[9] H.Kaushal and G.Kaddoum, "Underwater optical wireless communication," *IEEE Access*, vol. 4, pp. 1518–1547, 2016.

[10] F.Senel, "Coverage-aware connectivity-constrained unattended sensor deployment in underwater acoustic sensor networks,"*Wireless Communications and Mobile Computing*, vol. 16, no. 14, pp. 2052–2064, 2016.

[11] F.Senel, K. Akkaya, M. E. Kantarci, and T. Yilmaz, "Self-deployment of mobile underwater acoustic sensor networks for maximized coverage and guaranteed connectivity,"*Ad Hoc Networks*, vol. 34, pp. 170–183, 2015.

[12] A.Bahcebasi, V.C.Gungor, and G. Tuna, "Performance analysis of different modulation schemes for underwater acoustic communications,"in *Proc. 2018 3rd International Conference on Computer Science and Engineering (UBMK) IEEE*, pp. 396–401, 2016.

[13] S. Kim and J. Choi, "Optimal deployment of sensor nodes based on performance surface of underwater acoustic communication,"*Sensors*, vol. 17, no. 10, p. 2389, 2017.

[14] A. M. Ahmad, M.Barbeau, J. G. Alfaro, J. Kassem, and E. Kranakis, "Tuning the demodulation frequency based on a normalized trajectory model for mobile underwater acoustic communications,"*Transactions on Emerging Telecommunications Technologies*, vol. 30, no. 12, 2017.

[15] H. Nam, "AUV based data-gathering protocol for the lifetime extension of underwater acoustic sensor networks,"*IEICE Transactions on Fundamentals of Electronics, Communications and Computer Sciences*, vol. 100, no. 7, pp. 1596–1600, 2017.

[16] M. R.Bharamagoudra and S. S. Manvi, "Agent-based secure routing for underwater acoustic sensor networks," *International Journal of Communication Systems*, vol. 30, no. 13, 2017.

[17] H. Nam, "Data-gathering protocol-based AUV path-planning for long-duration cooperation in underwater acoustic sensor networks,"*IEEE Sensors Journal*, vol. 18, no. 21, pp. 8902–8912, 2018.

[18] Y.Liu*et al.*,"Error analysis of a distributed node positioning algorithm in underwater acoustic sensor networks,"in *Proc. 2018 10th International Conference on Wireless Communications and Signal Processing (WCSP) IEEE*, pp. 1–6, 2018.

[19] V.Sivakumar and D. Rekha, "Node scheduling problem in underwater acoustic sensor network using genetic algorithm,"*Personal and Ubiquitous Computing*, vol. 22, no. 5–6, pp. 951–959, 2018.

[20] P.Manasa and M.Ayyadurai, "Energy optimization using hybrid CAT-dolphin clustering algorithm in comparison with channel aware routing protocol," *ECS Transactions*, vol. 107, no. 1, p. 11981, 2022.

[21] M.Ayyadura*et al.*,"Hybrid atom search-heap energy optimization algorithm for dynamic topology in underwater acoustic sensor network," *International Journal on Devices, Circuits and Systems,* pp. 472–476, 2016.

[22] K. K.Gola and B. Gupta, "Void node avoidance in underwater acoustic sensor network using black widow optimization algorithm," *Adhoc and Sensor Wireless Networks*, vol. 52, 2012.

[23] R.Bhairavi and G. F. Sudha, "Energy efficient advancement-based dive and rise localization for underwater Acoustic sensor networks,"*Inventive Computation and Information Technologies*, pp. 241−255,2022.

[24] V.Sivakumar*et al.*,"Energy-efficient markov-based lifetime enhancement approach for underwater acoustic sensor network," *Journal of Sensors*, pp. 1−10,*2022.*

[25] S. P. Madheswari and V. S. Bhargavi, "Inter-intra cluster energy balance routing (I2cebr) protocol for underwater acoustic sensor networks using network coding," *International Journal of Modern Agriculture*, vol. 10, no. 3,pp. 157−168, 2021.

[26] Y.Chen*et al.*,"QMCR: A Q-learning-based multi-hop cooperative routing protocol for underwater acoustic sensor networks," *China Communications*, vol. 18, no. 8, pp. 24−236, 2021.

[27] G. J.Alqahtani and F. Bouabdallah, "Energy-efficient mobility prediction routing protocol for freely floating underwater acoustic sensor networks," *Frontiers in Communications and Networks*, vol. 2, p. 692002, 2021.

[28] D.Anuradha *et al.*, "Chaotic search-and-rescue-optimization-based multi-hop data transmission protocol for underwater wireless sensor networks," *Sensors*, vol. 22, no. 8,p. 2867, 2022.

[29] M.Faheem*et al*., "FFRP: Dynamic firefly mating optimization inspired energy efficient routing protocol for internet of underwater wireless sensor networks," *IEEE Access*, vol. 8, pp. 39587−39604, 2020.

[30] M. Faheem, G. Tuna, and V. C. Gungor, "QERP: Quality-of-service (QoS) aware evolutionary routing protocol for underwater wireless sensor networks," *IEEE Syst. J.*, vol. 12, no. 3, pp. 2066−2073, Sep. 2018.